ENVIRONMENTAL MICROBIOLOGY

Electroactivity of Phototrophic River Biofilms and Constitutive Cultivable Bacteria

Running Title: Electroactive river biofilm and bacteria

Keywords: bacterial population, bacterial community, electroactivity, epilithic biofilm, oxygen reduction.

Emilie Lyautey,[1,2†] Amandine Cournet,[3] Soizic Morin,[4] Stéphanie Boulêtreau,[1,2] Luc Etcheverry,[5] Jean-Yves Charcosset,[1,2] François Delmas,[4] Alain Bergel[5] and Frédéric Garabétian[6*]

Université de Toulouse, UPS, INP, Laboratoire d'Ecologie fonctionnelle, 118 route de Narbonne, F-31062 Toulouse, France[1]; CNRS, EcoLab, F-31062 Toulouse, France[2]; Université de Toulouse, UPS, LU49, Adhésion bactérienne et formation de biofilms, 35 chemin des Maraîchers, F-31062 Toulouse, France[3]; Cemagref, UR REBX, 50 avenue de Verdun, F-33612 Cestas, France[4]; Université de Toulouse, Laboratoire de Génie Chimique, 4 allée Emile Monso, F-31030 Toulouse, France[5]; Université de Bordeaux, Environnements et Paléoenvironnements Océaniques, Bordeaux, F-33000, France[6]

[*]Corresponding author. Mailing address: Université de Bordeaux, EPOC UMR 5805 / OASU, Station Marine d'Arcachon, 2 rue Jolyet, F-33120 Arcachon Cedex, France. Phone: 33 5 5622 3909. Fax: 33 5 5683 5104. E-mail: f.garabetian@epoc.u-bordeaux1.fr.

[†] Present address: Université de Savoie, UMR 42 CARRTEL, F-73376 Le Bourget du Lac.

ABSTRACT

Electroactivity is a property of biofilm assembled microorganisms that has been highlighted in a variety of environments. This characteristic was assessed on phototrophic river biofilms at the community and at the bacterial population scale. At the community scale, electroactivity was evaluated on stainless steel and copper alloy coupons used both as biofilm colonization supports and working electrodes. At the population scale, the ability of environmental bacterial strains to catalyze oxygen reduction was assessed by cyclic voltammetry. Our data demonstrated that phototrophic river biofilms development on the electrodes, supported by dry mass and Chlorophyll *a* content, resulted in significant increase of the recorded potentials, with potential up to +120 mV/SCE on stainless steel and +60 mV/SCE on copper electrodes. Thirty two bacterial strains isolated from natural phototrophic river biofilms were tested by cyclic voltammetry. Twenty five were able to catalyze oxygen reduction with a shift of potential ranging from 0.06 to 0.23 V, cathodic peak potentials from –0.36 to –0.76 V/SCE and amplitudes from –9.5 to –19.4 µA. These isolates were phylogenetically diversified (*Actinobacteria, Firmicutes*, *Bacteroidetes*, α-, β-, and γ-*Proteobacteria*) and exhibited various phenotypical properties (Gram, oxidase and catalase characteristics). This data suggests that phototrophic river biofilms communities and/or most of the constitutive bacterial populations present the ability to promote electronic exchange with a metallic electrode supporting the following perspectives: (i) develop electrochemistry-based sensors allowing *in situ* phototrophic river biofilms detection and (ii) produce microbial fuel cell inoculum in oligotrophic conditions.

Biofilm assembled microorganisms present several properties out of which arises electroactivity, the ability to catalyze electron transfers between cells and their support (37). Biofilm bacterial cell electroactivity has many implications in industrial and environmental domains, such as biocorrosion (33), microbial fuel cells (MFC; 36, 52), and biofilm or pollution detection (3, 46, 60).

Oxidation reactions, i.e. electron transfer from the biofilm to the electrode, are well documented and attributed to ferri-reducing bacteria such as *Geobacter sulfurreducens* or *Shewanella putrefaciens*, capable of directly interacting with their solid support through periplasmic cytochromes or membrane proteins (5, 29), or through the occurrence of bacterial geopili (nanowires; 22). The investigation of various environments found electroactive microbial communities in marine sediments, activated sludge, compost communities, or soils (36).

Community electroactivity was first identified in the reduction direction with the electrode serving as electron donor. The catalysis of oxygen reduction by marine bacteria was the first identified example of electron transfer from a metallic material to biofilm-assembled microorganisms (45, 56). So-called biocathodes received an increasing interest, widening the final electron acceptor to different compounds such as sulphate, nitrate or fumarate (26, 54, 64). Understanding the biocathode mechanisms remains a hot research topic and the catalysis of oxygen reduction on metallic electrodes by attached marine bacteria is still investigated (17, 18, 20, 51). Catalysis of oxygen reduction was also demonstrated in drinking water (15) and several aerobic genera exhibited abilities to catalyze oxygen reduction on solid electrodes (13, 51). However, few studies revealed such electroactivity properties for surface water ecosystem microbial communities, and focused only on sediment communities (23, 27, 47).

In river hydrosystems, typical microorganism assemblages are phototrophic river biofilms (PRB) colonizing the interface between the river bottom and the water column, and composed of

algae, bacteria and other microorganisms (35). The objectives of the present study were to: (i) *in situ* assess the ability to promote electronic exchange with a metallic electrode by recording the potential of submerged metallic supports colonized by PRB during colonization experiments, (ii) assess the relationship between *in situ* electrochemical potentials and diatom and bacterial community structure for PRB assemblages grown on two metallic supports, and (iii) screen PRB bacterial isolates to determine their individual electrochemical activity using a voltammetric technique sensitive to detect bacterial strain electroactivity with respect to oxygen reduction.

MATERIALS AND METHODS

Study sites. PRB were collected in two French hydro-ecoregions (HER, 63). Site S (corresponding to site 336; 61), located at Saillant on the Vézère River proper (Dordogne, France), is 20 km upstream of Brive-la-Gaillarde. At this site, located in the HER 21 "Massif Central Nord", average water pH is 7, conductivity is below 200 µS cm^{-1} (granitic substrate), river is 20 m wide, and water depth on the pebble reach is about 50 cm. Site U1 (40), located at l'Aouach on the Garonne River proper (Haute-Garonne, France), is 30 km upstream of Toulouse metropolitan area. At this site, located in the HER 14 "Coteaux Aquitains", average water pH is 8.1, average conductivity is 350 µS cm^{-1}, river is 60 m wide, and water depth is about 1 m on the pebble reach. At both sites, river waters are well oxygenated (> 90 %) and average NO_3^- and SO_4^{2-} concentrations are around 0.01 and 0.2 mM at U1 and around 0.1 and 0.4 mM at D2, respectively.

Community level monitoring of electrochemical PRB. *In situ* PRB monitoring was carried out at site U1 in 2006 and 2007. Metallic slides (100 × 25 × 1 mm) were used as electrodes and colonization supports. They were maintained in a vertical position, parallel to the flow, within a stainless steel rack anchored to the river bottom close to the river bank. The potential of each

electrode was monitored against a saturated calomel reference electrode (SCE) using a multichannel datalogger (16-channels Datahog2, Skye Instruments, UK). Electrodes were made of stainless steel (n = 4) and copper (n = 2) alloys and were immerged in the river for 35 days in 2006 and for 18 days in 2007. In order to ensure our data was not skewed by biofouling issues, control experiments were run using a second reference electrode at the same time; with no significant difference recorded, this indicates that the reference electrode was only marginally disturbed by biofouling (data not shown).

Biofilm collection and biomass measurements. PRB grown both on artificial (electrodes) and natural (pebbles) supports were collected. Artificial PRB were collected in November 2006 and November 2007 and natural PRB (nine colonized pebbles) were collected on September 30, 2008 at site U1, and on October 1, 2008 at site S. Samples were kept at 4°C during transport to the laboratory and biofilm conditioning was initiated within 6 h of sampling. PRB were aseptically removed from their substrata using a toothbrush (treated with 1N NaOH) and suspended in 0.2 µm filter-sterilized water. Dry mass (DM) and chlorophyll *a* (Chl *a*) concentration were measured from PRB suspensions according to the protocols previously described (43). Briefly, DM was determined by weighing dried PRB (105°C) and Chl. *a* was determined using trichromatic spectrophotometric equations (28).

Bacterial community composition analysis. Bacterial community composition analysis was carried out on PRB grown on natural and artificial supports. DNA extraction was carried out on aliquots (50 mg DM for biofilms grown on pebbles and from 0.1 to 15.6 mg DM for biofilms grown on metallic slides) of the biofilm suspensions using Mobio UltraClean Soil DNA Isolation kits according to the manufacturer's protocol. For practical reasons, two distinct fingerprinting techniques were used. Bacterial community composition was studied using a 16S-based PCR-DGGE approach (42) for biofilms grown on metallic electrodes in year 2006. For biofilms grown

on electrodes in 2007 and for biofilms grown on pebbles collected in 2008, bacterial community composition was assessed using Automated Ribosomal Intergenic Spacer Analysis (ARISA). It is unlikely that DGGE indicate differences that could not be detected by ARISA since both fingerprinting techniques are considered suitable for studying bacterial community diversity at the species level. As ARISA is more sensitive than DGGE and generally detects more OTUs, care was taken of presenting both method results separately since raw data are not directly comparable, although data interpretations are likely comparable. PCR amplification of the 16S-23S rDNA intergenic spacer was carried out using 5'FAM labelled S-D-Bact-1522-B-S-20 and L-D-Bact-132-a-A-18 primers (49). The final reaction mix (25 µl) consisted of 1× PCR buffer (Promega, Charbonnières, France), 1.5 mM $MgCl_2$, 0.3 mg ml^{-1} bovine serum albumine, 5% DMSO, 200 µM of each deoxynucleoside triphosphate (Eurogentec, Seraing, Belgium), 0.5 µM of each primer (Invitrogen, Cergy Pontoise, France), 0.25U of *Taq* polymerase (Promega) and 50 ng of DNA. Amplification was performed with a Mastercyler (Eppendorf, Le Pecq, France): after an initial denaturation at 94ºC for 5 min, 35 cycles of denaturation (94ºC, 1 min), annealing (55ºC, 1 min) and extension (72ºC, 1 min) were performed, followed by a final extension (72ºC, 10 min). Amplification products were quantified on 1.65% gel agarose using Mass Ruler Express DNA Ladder, LR forward (Fermentas, Saint Rémy les Chevreuses, France) and diluted to a final concentration of 10 ng μl^{-1}. Finally, 2 µl of diluted product was mixed with 0.5 µl GeneScan 1200 LIZ internal size standard (Applied Biosystems, Courtaboeuf, France) and 9 µl Hi-Di formamide (Applied Biosystems), and the mixture was denatured at 95°C for 3 min. Fragments were discriminated using an ABI 3100 automated sequencer (Plateau de génomique, IFR 150, Toulouse, France) and the resulting electropherograms analysed using the Applied Biosystems Peak Scanner software. Peaks contributing < 0.1% of the total amplified DNA (as determined by relative fluorescence intensity) were eliminated from profiles as being indistinguishable from

baseline noise (25). Peaks or bands were scored as present or absent from DGGE and ARISA analyses. Similarity between profiles was computed from the Jaccard similarity index.

Algal community composition analysis. Algal community composition was studied on PRB collected on metallic electrodes in 2006 and 2007. After removal from the supports, biofilms were suspended into a standard volume of mineral water, preserved within a formalin solution before taxonomic identification. Samples were prepared according to the European standard NF EN 13946 and deposited onto coverslips then mounted onto slides after air drying, using the high refractive index (1.74) medium Naphrax (Brunel Microscopes Ltd, UK). Diatom counts were conducted at a magnification of 1000 ×; individual fields were scanned until at least 400 valves had been identified using taxonomic literature from central Europe (30) and recent nomenclature updates.

Isolation of bacterial strains from PRB. Bacterial strains were isolated from PRB grown on natural support and collected in 2008 at sites U1 and S as biofilm glycerol stocks from the 2006 and 2007 field campaigns failed to yield to any colonies. The cultivable portion of bacteria in PRB was assessed either using direct plating or following enrichment. For the direct plating approach, 100-µl portions of serial dilutions of the biofilm suspensions were inoculated on full strength Tryptone Soy agar (TSA; Sigma-Adrich, Lyon, France), 10 times diluted TSA, full strength Nutrient Agar (NA; Sigma-Aldrich) and 10 times diluted NA. Plates were incubated aerobically for 5 days at 20°C. Colonies were picked up and subsequently streaked on the corresponding agar medium (3 times) to obtain well isolated colonies. For the enrichment approach, 5-ml portions of the biofilm suspensions were inoculated into 45 ml of full strength Tryptone Soy Broth (TSB; Sigma-Aldrich), 10 times diluted TSB, full strength Nutrient Broth (NB; Sigma-Aldrich) and 10 times diluted NB, and incubated aerobically for 10 days at 20°C under agitation (50 rpm). One hundred-µl portions of enrichments were subsequently plated onto

the corresponding agar media and incubated aerobically for 5 days at 20°C. Colonies were isolated using the protocol described above. Isolated colonies were inoculated into sterile 96-well plates containing 100 µl well^{-1} of the broth corresponding to the media used for isolation, and incubated 24 to 48 h at 20°C. Sterile glycerol was added to each well at a final concentration of 20% (v/v), and the plates were stored at –80°C.

PCR-RFLP typing and 16S rDNA sequencing of bacterial strains. The bacterial collection (n = 246 and 225 strains for site U1 and S, respectively) was characterized by *Hae*III restriction fragment length polymorphism (RFLP) of the 16S rDNA fragment. Bacterial isolate fresh cell suspensions (100 µl, using the isolation broth) were pelleted by centrifugation (2500 × g for 25 min; Heraeus Multifuge, Thermo Fisher Scientific, Courtaboeuf, France), resuspended in 100 µl sterile 100 mM Tris-HCl, and lysed using a heat-shock procedure. Cell lysates were pelleted by centrifugation at 4100 × g for 10 min. The final reaction mix (25 µl) consisted of 1× PCR buffer (Promega), 1.5 mM $MgCl_2$, 0.3 mg ml^{-1} bovine serum albumine, 200 µM of each deoxynucleoside triphosphate (Eurogentec), 0.5 µM of each 27F and 1492R primer (Invitrogen; Lane, 1991), 1.25U of *Taq* polymerase (Promega) and 5 µl of lysate supernatant as template. Amplification was performed with a Mastercycler: after an initial denaturation at 95ºC for 4 min, 35 cycles of denaturation (94ºC, 1 min), annealing (55ºC, 1 min) and extension (72ºC, 2 min) were performed, followed by a final extension (72ºC, 15 min). Amplified DNA (1 µg) was digested using 5U of *Hae*III enzyme (Promega) for 4 h at 37°C. PCR-RFLP fragments were separated by electrophoresis (2.5 h, 100 V) on a 3% agarose gel (Sigma-Aldrich). Gels were stained with ethidium bromide and images were captured as 16-bit TIFF images using CCD camera and Biocapt Software (Vilbert Lourmat, Marne-la-Vallée, France). Normalization of gel images and assignment of PCR-RFLP fingerprints to isolates were done with the BioNumerics software package (version 5; Applied Maths, Kortrijk, Belgium). The assignment of strains to

different clusters was performed by calculating the similarity coefficients with the curve-based Pearson similarity coefficient. Similarity trees were generated using the unweighted-pair group method using average linkage. PCR-RFLP clusters were initially assigned using the software and the final assignments were determined on the basis of careful visual inspection.

Sequencing of the amplified 16S rDNA products was carried out by Macrogen (Korea) using primers 27F and 1492R. Sequence analysis and phylogenetic trees construction were done using the Ribosomal Database Project release 10, update 12 (10). Sequences were aligned using the RDP aligner and the phylogenetic tree was constructed using the Tree Builder tool, and imported into the online UniFrac interface (38, 39) to specifically test for differences among the two sites diversity based on phylogenetic relationships. A total number of 45 partial 16S rDNA sequences have been deposited in the GenBank sequence database under accession numbers GQ398331 to GC398375 (Table 1).

Cyclic voltammetry. A subset of 32 sequenced strains, chosen to represent a maximal phylogenetic diversity, was tested by cyclic voltammetry to assess their capacity to catalyze oxygen reduction on a carbon electrode. Bacterial isolates were cultivated in TSB (60 ml) at 20°C, under agitation (150 rpm) for 24 h. Cells were harvested by centrifugation (3400 g, 10 min, 4°C, Heraeus Multifuge), and rinsed twice with 2 ml 0.1 M potassium phosphate (K_2HPO_4/ KH_2PO_4, v/v) buffered at pH 7.0 to obtain the final working bacterial cell suspension. Cyclic voltammetry was performed at 100 mV s^{-1} at ambient temperature with a multipotentiostat (VMP2 Bio-Logic SA, France). A three-electrode system was used in a 100 ml beaker with a saturated calomel electrode (SCE) as reference and a platinum wire (0.5 mm diameter) as counter electrode. A glassy carbon (GC) rod (V25, 3 × 150 mm, Carbone Lorraine, France) was used as working electrode, and was inserted in insulating resin to obtain disk electrodes of 3 mm diameter. The electrodes were polished with abrasive silicon carbide paper of decreasing grit size

(P120 to P4000, LAM-PLAN, France) and cleaned in distilled water before each electrochemical experiment. The potential scan started from the open circuit potential and progressed towards the upper limit, in the range –1.00 to 0.70 V/SCE. The standard CV procedure was composed of 4 steps set in the electrochemical cell without moving the electrodes: (i) CV1 was performed in 30 ml sodium phosphate buffer (NaH_2PO_4) 0.1 M at pH 7.5, (ii) CV2 was performed directly after addition of the adequate volume of bacterial cell suspension in the buffer solution to obtain a working OD of 0.8, (iii) the electrode was kept in the bacterial cell suspension, stirred with a Teflon coated magnetic stirrer, for 1 to 3 hrs before (iv) CV3 was recorded. In order to compare the effectiveness of the catalysis of oxygen reduction among the different experiments (no other alternative electron acceptors such as nitrate or sulphate was available in the buffer), the potential shift was measured at a constant value of current, arbitrarily chosen at –6 μA, for all voltammograms.

Phenotypic characterization of bacterial strains. The 32 isolates tested in cyclic voltammetry were examined for Gram staining, oxidase and catalase expression according to standard procedures (21). Briefly, an isolated colony recovered after 24 to 36 h of growth at 20°C on TSA was tested for Gram reaction (kit Color Gram 2, Biomerieux, France), N-méthyl-paraphenylene diamine oxidation (Ox disks, Bio-Rad, France) and catalysis of hydrogen peroxide transformation to di-oxygen and water of a 3% (w/v) medical solution (Gifrer, France) by suspending the colony in sterile physiologic water on a microscopic slide.

Data analysis. Mann-Whitney test was used to compare electrochemical potentials, biomass descriptors, and bacterial population phenotypic characteristics. Changes in the bacterial and diatom community compositions were analysed by multidimensional scaling (MDS) according to a procedure described previously (2). MDS distances are based on Jaccard similarity index, calculated on presence-absence of diatom and bacterial populations. Statistical differences

between groups determined from the MDS plot were tested using random permutation test (Monte-Carlo test, 100,000 permutations) as described previously (31) and using the stand alone program provided by the authors.

RESULTS

Electrochemical PRB monitoring. *In situ* electrochemical potential significantly increased during the first 10 days of colonization, and then remained substantially constant, irrespective of the year, for PRB grown on copper or stainless steel electrodes (Fig. 1). In 2006, after 35 days of development, copper-grown biofilms exhibiting lower potentials (around –70 mV/SCE) than stainless steel-grown biofilms (around +120 mV/SCE). In 2007, after 10 days of development, electrochemical potentials reached a plateau both on stainless steel and copper electrodes, but unlike year 2006, no clear difference was observed between stainless steel-grown (around +80 mV/SCE) and copper-grown biofilms (around +60 mV/SCE) potentials after 18 days of development. Both for 2006 and 2007 experiments and independently of the support used, no significant difference was observed between day and night electrochemical potentials.

Biomass, diatom and bacterial community structure of PRB grown on metallic supports. In 2006, biomass recorded on stainless steel and copper electrodes were not significantly different when expressed as DM (average ± s.d.) (1.25 ± 0.48 and 1.29 ± 0.52 mg cm^{-2} for stainless steel and copper electrodes, respectively; Mann-Whitney test, $P = 0.93$), but were significantly different when expressed as Chl. *a* (1.31 ± 0.20 and 0.27 ± 0.36 µg cm^{-2} for stainless steel and copper electrodes, respectively; Mann-Whitney test, $P < 0.01$). In 2007, no significant difference was observed for DM (1.15 ± 0.56 and 0.22 ± 0.21 mg cm^{-2} for stainless steel and copper electrodes, respectively; Mann-Whitney test, $P = 0.09$) or Chl. *a* (4.29 ± 1.67

and 0.45 ± 0.04 µg cm^{-2} for stainless steel and copper electrodes, respectively; Mann-Whitney test, $P = 0.054$).

For diatom community, richness (S) ranged between 60 and 71 species in 2006 (65 ± 2 and 65 ± 8 species for stainless steel and copper electrodes, respectively) and between 38 and 45 species in 2007 (41 ± 1 and 41 ± 5 species for stainless steel and copper electrodes, respectively). A total of 141 species were identified but the communities were dominated by the following species: *Achnanthidium pyrenaicum* (Hustedt) Kobayasi (15.4 ± 1.2%), *Encyonema minutum* (Hilse in Rabhenhorst) D.G. Mann (13.5 ± 0.8%), *Nitzschia dissipata* (Kützing) Grunow var. *dissipata* (9.8 ± 1.4%) and *Melosira varians* Agardh (9.6 ± 1.8%). Two-dimension MDS representation of community composition allowed discriminating diatom communities based on the year of sampling rather than on the metallic support used (Fig. 2a). Average similarity values for communities within the same year were 52% and 57% for 2006 and 2007, respectively. Between years, similarity value was 38%. Average similarity values for communities from the same metallic support were 47% and 43% for stainless steel and copper, respectively, whereas between metallic supports, similarity value was 44%. Based on Monte-Carlo permutation test, 2006 and 2007 communities were significantly differentiated ($P < 0.005$), whereas within each year stainless steel and copper grown communities exhibited only marginally significant differences ($P < 0.1$ for both 2006 and 2007 communities).

For bacterial community, in 2006, richness (S) ranged between 26 and 36 OTU's (29 ± 3 and 31 ± 6 OTU's on stainless steel and copper electrodes, respectively). Two-dimension MDS discriminated bacterial communities on the metallic support used, and Monte-Carlo permutation test demonstrated that the difference was significant ($P < 0.001$) (Fig. 2b). Average similarity values for communities from the same metallic support were 60% and 43% for stainless steel and copper, respectively, whereas between metallic supports, similarity value was 39%. In 2007,

richness (S) ranged between 57 and 99 OTU's (81 ± 18 and 74 ± 3 OTU's on stainless steel and copper electrodes, respectively). Two-dimension MDS did not allow discrimination of bacterial communities on the metallic substrata used (Fig. 2c). Average similarity values for communities from the same metallic support were 32% and 58% for stainless steel and copper, respectively, whereas between metallic supports, similarity value was 35%.

Molecular- and culture-based phototrophic river bacterial diversity. Site U1 and S communities ARISA profiles yielded to 147 different peaks ranging from 200 to 671 bp (Fig. 3). Site U1 community exhibited 97 peaks from 200 to 653 bp, and site S community exhibited 97 peaks ranging from 200 to 671 bp. The similarity value between the two communities was 25%.

Based on *Hae*III PCR-RFLP analyses, the 246 and 225 bacterial strains isolated were discriminated into 16 and 35 ribotypes for U1 and S communities, respectively. The nearly full 16S rDNA gene (~ 1400 bases) of representative bacterial strains from these 51 ribotypes was sequenced. Phylogenetic analyses were performed on the 45 good quality sequences (15 for U1 and 30 for S). Eleven and six sequences were related to the Gram-positive *Actinobacteria* and *Firmicutes*, respectively. Four sequences were related to *Bacteroidetes*, and six, four and fourteen sequences were related to α-, β-, and γ-*Proteobacteria* (see Fig. S1 in the supplemental material). The pairwise UniFrac significance test probability for the site U1 and site S communities was 0.73 indicating that there was no significant difference ($P < 0.1$) between the two bacterial communities.

Electrochemical activity of phototrophic river bacterial strains. Typical cyclic voltamogramms of oxygen reduction catalyzed by three bacterial isolates are shown Fig. 4. The values obtained for the shift of potential, peak amplitude and peak potential for the 32 bacterial isolates, along with their Gram, catalase and oxidase properties, are indicated in Table 1. Gram staining showed discrepancies between the expected and the obtained response for 9 out of 32

strains that were tested. Seven isolates yielded to results indicating that they were not able to catalyze oxygen reductions. The 25 remaining isolates were able to reduce oxygen reduction with varying catalytic effect. For these isolates, bacterial cells catalyzed the oxygen reduction with a shift of potential ranging from 0.06 to 0.23 V/SCE at –6 µA (n = 25). Four isolates had small catalytic effects, as they induced potential shifts but no clear peak. Peak potentials ranged from –0.36 to –0.76 V/SCE and amplitudes ranged from –9.5 to –19.4 µA (n = 21). No difference was observed for shift of potential, peak potential and peak amplitude value distributions between Gram-negative and Gram-positive bacterial isolates, between catalase-negative and catalase-positive bacterial isolates, or between oxidase-negative and oxidase-positive bacterial isolates (Mann-Whitney test, P-values > 0.05).

DISCUSSION

In the present work, we demonstrated that PRB from two different HER were able to generate electrochemical potential increase that stabilized during their development. Such a potential increase was first identified in seawater and was attributed to the catalysis of oxygen reduction by biofilm-assembled marine bacteria (56). The open circuit potential (OCP, i.e. the potential that takes a conductive material out of any artificial control) is controlled by the balance between the spontaneous oxidation/reduction reactions occurring between the material surface and the chemical species dissolved in the liquid environment. Increasing the rate of oxygen reduction enhances the rate of electron extraction from the material, which induces an OCP increase. The voltammetric investigations implemented on the aerobic cultivable bacterial populations isolated from these PRB confirmed that more than half of the tested isolates presented the capacity to catalyze the electrochemical reduction of oxygen.

At the community scale, the submersion of metallic electrodes used as supports yielded to characteristic PRB biomass as demonstrated by DM and Chl. *a* measurements that compared to natural assemblage biomass (41). Even though the artificial nature of the supports used was likely to influence community compositions (9), year 2006 diatom community structure from metallic supports exhibited similarities of more than 80% with communities from pebble assemblages simultaneously collected (data not shown), demonstrating that realistic PRB communities were studied. Significant differences in Chl. *a* content, diatom and bacterial community composition were observed between copper- and stainless steel-grown PRB, and these observations are consistent with previous observations demonstrating the sensitivity of PRB communities to copper exposure (1, 4, 55). The differences observed between 2006 and 2007 experiment should be interpreted as a climate-dependent interannual variability (e.g. river flow regime).

Along with PRB colonization and development, metallic electrodes allowed the observation of significant increase of electrochemical potentials, reaching a plateau in the range of +80 to +120 mV/SCE for stainless steel and of –70 to +60 mV/SCE for copper electrodes, comparable with those obtained for lotic freshwater biofilms on stainless steel supports (19, 44). Mechanisms reported to be responsible for electrochemical potential increase are: production by biofilm microorganisms of oxidizing agents through enzyme catalysis, eg. H_2O_2 or Mn-oxide in manganese-rich environments; modification of the composition of the oxide layer of stainless steel; production of some compounds that adsorb on the material surface and play the role of electro-catalyst (33). If electroactivity is mainly described for bacterial strains, previous studies demonstrated that algae were also involved (34, 48), causing day / night fluctuation of the electrochemical potential recorded on stainless steel (44). Algae, through photosynthesis, would modify the local production of O_2, contributing to an increase of the recorded electrochemical potentials during photosynthesis periods. Numerous couplings between algae and electro-

catalytic microbial biofilms were recently described in the field of MFC. The objective is to use the organic compounds produced by the algae as substrate for the MFC, designing photosynthetic algal MFC (53, 57). In photosynthetic MFC the main electron pathway has no direct link with catalysis of oxygen reduction, since algae are used to produce the substrate that is oxidized on the anaerobic bioanode, even if some effect of oxygen has been claimed (24). The decrease in current provided by the MFC that was observed in the light was attributed to the production of oxygen via photosynthesis: oxygen impeded the anaerobic reactions that take place on the bioanode. Authors proposed to use this phenomenon to design reversible algal photosynthetic bioelectrodes behaving as anodes in dark periods and reversing to cathodes under illumination because of algal oxygen production (58). In the present work, such a coupling on the cathode would have enhanced the current due to oxygen reduction and resulted in OCP increase, but no obvious trend between day and light periods was observed. The electrodes used here being positioned vertically in the river, this could have limited PRB exposure to light and the observation of contrasted night and day potentials. Lower electrochemical potentials were observed on copper electrodes along with lower chlorophyll content, possibly due to copper exposure affecting photosynthesis activities (55), although other mechanisms involving the competition between algae and bacteria for nutrients or substrates might be involved. The use of PRB could represent an interesting alternative to circumvent one the main drawback of MFC technology: the limiting performance of the cathode, shown to be related to the decreasing diffusion of O_2 to the inner layers of bacterial biofilms. Several options were proposed to improve the oxygen transfer: use of pure oxygen, pressurized air or photosynthetic microorganisms (8, 59), and PRB would represent an interesting compromise given their ability to be involved in bacterial oxygen reduction and being composed of an important photoautrophic community that would favor oxygen production and diffusion.

By sampling natural biofilms from two different hydroecoregions, we sought to isolate differentiated bacterial populations. Molecular-based fingerprint analyses confirmed that bacterial communities from the two sites were different, but the phylogenetic diversity of the cultivable fraction recovered was not different, probably due to the unavoidable selective effect of culture (11). However, the bacterial strains isolated were diversified and belong to commonly reported phylogenetic groups for this kind of assemblage (7), but discrepancies between phenotypic characteristics and phylogenetic identification suggest that strain affiliation could be more accurately defined. Shift of potential, peak amplitude and peak potential were in the range of those observed for bacterial strains isolated from seawater biofilms and reference or clinical strains using the same approach (13, 50, 51). The strains shown to be able to catalyze the electrochemical reduction of oxygen were not only belonging to different phylogenetic groups, but were also either Gram-, catalase- and oxidase-positive or negative, confirming recent outcomes (13, 62). Different mechanisms were proposed to explain microbially catalyzed reductions: direct catalysis by adsorbed enzymes like catalase (32), indirect catalysis through the production of hydrogen hydroxide (16) or production of manganese oxides/hydroxides by manganese oxidizing bacterium (14). Understanding the exact mechanisms involved for our bacterial strains (*e.g.* presence of membrane-bound compounds or extracellular compounds; 13) would have required to perform further testing not carried out. However, previous studies demonstrated that, even if it is not the sole mechanism involved, bacterial adhesion on the electrode surface was needed and the involvement of porphyrin compounds has been strongly suspected (12).

The present work demonstrated that PRB shared the same traits than other electroactive aggregates from other environments and present the ability to promote electronic exchange with a metallic electrode thereby forming a biocathode. This property was highlighted both at the

community and at the population scale although interannual variations might limit the generalization of the findings. At the community scale, this opens perspectives towards the detection and continuous growth monitoring of such assemblages in freshwater, as an alternative to other electrochemical techniques (6). At the population scale, this proves that such biofilms are also composed of electroactive individual bacterial populations enriching the set of electroactive bacterial strains and suggesting that electroactivity likely results from the assembling of adjacent cells onto a surface representing an emergent property of microorganisms assembled in biofilms. With the growing interest in photosynthetic MFC, PRB which can be easily collected in rivers worldwide could represent good candidates for the production of MFC inoculum.

ACKNOWLEDGMENTS

This work is a part of the project SurF "*Surveillance des rivières par les biofilms*" funded by CNRS PNIR "Biofilms", Région Midi-Pyrénées and Région Aquitaine (*action interrégionale Aquitaine & Midi-Pyrénées*). EL was supported by a postdoctoral fellowship from the Région Midi-Pyrénées and SM by a postdoctoral fellowship from the Région Aquitaine.

We thank L. Bourasseau for technical assistance with bacterial strains phenotypic characterization. D. Féron and M. Roy from CEA-Saclay (DEN/SCCME) are gratefully thanked for providing the metal samples and the rack used for exposure experiments in rivers.

REFERENCES

1. **Ancion, P. Y., G. Lear, and G. D. Lewis.** 2010. Three common metal contaminants of urban runoff (Zn, Cu & Pb) accumulate in freshwater biofilm and modify embedded bacterial communities. Environ. Pollut. **158**:2738–2745.
2. **Araya, R., K. Tani, T. Takagi, N. Yamaguchi, and M. Nasu.** 2003. Bacterial activity and community composition in stream water and biofilm from an urban river determined by fluorescent *in situ* hybridization and DGGE analysis. FEMS Microbiol. Ecol. **43**:111–119.
3. **Atekwana, E. A., E. A. Atekwana, D. D. Werkema, J. P. Allen, L. A. Smart, J. W. Duris, D. P. Cassidy, W. A. Sauck, and S. Rossbach.** 2004. Evidence for microbial enhanced electrical conductivity in hydrocarbon-contaminated sediments. Geophys. Res. Lett. **31**:L23501–L23504.
4. **Boivin, M. Y., B. Massieux, A. M. Breure, F. P. van den Ende, G. D. Greve, M. Rutgers, and W. Admiraal.** 2005. Effects of copper and temperature on aquatic bacterial communities. Aquat. Toxicol. **71**:345–356.
5. **Bond, D. R., D. E. Holmes, L. M. Tender, and D. R. Lovley.** 2002. Electrode-reducing microorganisms that harvest energy from marine sediments. Science **295**:483–485.
6. **Boulêtreau, S., J. Y. Charcosset, J. Gamby, E. Lyautey, S. Mastrorillo, F. Azémar, F. Moulin, B. Tribollet, and F. Garabetian.** 2011. Rotating disk electrodes to assess river biofilm thickness and elasticity. Water Res. **45**:1347–1357.
7. **Brümmer, I. H. M., W. Fehr, and I. Wagner-Döbler.** 2000. Biofilm community structure in polluted rivers: abundance of dominant phylogenetic groups over a complete annual cycle. Appl. Environ. Microbiol. **66**:3078–3082.

8. **Cao, X., X. Huang, N. Boon, P. Liang, and M. Fan.** 2008. Electricity generation by an enriched phtototrophic consortium in a microbial fuel cell. Electrochem. Comm. **10**:1392–1395.
9. **Cattaneo, A., and M. C. Amireault.** 1992. How artificial are artificial substrata for periphyton? J. N. Am. Benthol. Soc. **11**:244–256.
10. **Cole, J. R., Q. Wang, E. Cardenas, J. Fish, B. Chai, R. J. Farris, A. S. Kulam-Syed-Mohideen, D. M. McGarrell, T. Marsh, G. M. Garrity, and J. M. Tiedje.** 2009. The Ribosomal Database Project: improved alignments and new tools for rRNA analysis. Nucleic Acids Res. **37** (Database issue):D141–D145.
11. **Colwell, R. R., and D. J. Grimes.** 2000. Non culturable microorganisms in the environment. Chapman & Hall, London, UK.
12. **Cournet, A., M. Bergé, C. Roques, A. Bergel, and M. L. Délia.** 2010. Electrochemical reduction of oxygen catalyzed by *Pseudomonas aeruginosa*. Electrochim. Acta **17**:4902–4908.
13. **Cournet, A., M. L. Délia, A. Bergel, C. Roques, and M. Bergé.** 2010. Electrochemical reduction of oxygen catalyzed by a wide range of bacteria including Gram-positive. Electrochem. Commun. **12**:505–508.
14. **Dickinson, W. H., and Z. Lewandowski.** 1996. Manganese biofouling and the corrosion behavior of stainless steel. Biofouling **10**:79.
15. **Dulon, S., S. Parot, M. L. Délia, and A. Bergel.** 2007. Electroactive biofilms: new means for electrochemistry. J. Appl. Electrochem. **37**:173–179.
16. **Dupont, I., D. Féron, and G. Novel.** 1998. Effect of glucose oxidase activity on corrosion potential of stainless steels in seawaters. Int. Biodeter. Biodegrad. **41**:13–18.

17. **Erable, B., I. Vandecandelaere, M. Faimali, M. L. Délia, L. Etcheverry, P. Vandamme, and A. Bergel.** 2010. Marine biofilm in laboratory closed-systems. Bioelectrochem. **78**:30–38.

18. **Faimali, M., E. Chelossi, G. Pavanello, A. Benedetti, I. Vandecandelaere, P. De Vos, P. Vandamme, and A. Mollica.** 2010. Electrochemical activity and bacterial diversity of natural marine biofilm. Bioelectrochem. **78**:51–56.

19. **Féron, D., and M. Roy.** 2000. Corrosion behaviour of stainless steel in natural waters: focus on microbiological and chemical aspects. Proceedings of Eurocorr'.

20. **Freguia, S., S. Tsujimura, and K. Kano.** 2010. Electron transfer pathway in microbial oxygen biocathodes. Electrochim. Acta **55**:813–818.

21. **Gerhardt, P., R. G. E. Murray, W. A. Wood, and N. R. Krieg.** 1994. Methods for general and molecular bacteriology. American Society for Microbiology, Washington, DC.

22. **Gralnick, J. A., and D. K. Newman.** 2007. Extracellular respiration. Mol. Microbiol. **65**:1–11.

23. **He, Z., H. Shao, and L. T. Angenent.** 2007. Increased power production from a sediment microbial fuel cell with a rotating cathode. Biosens. Bioelectr. **22**:3252–3255.

24. **He, Z., J. Kan, F. Mansfeld, L. T. Angenent, and K. H. Nealson.** 2009. Self-sustained phototrophic microbial fuel cells based on the synergistic cooperation between photosynthetic microorganisms and heterotrophic bacteria. Env. Sci. Technol. **43**:1648–1654.

25. **Hewson, I., and J. A. Fuhrman.** 2004. Bacterioplankton species richness and diversity along an estuarine gradient in Moreton Bay, Australia. Appl. Environ. Microbiol. **70**:3425–3433.

26. **Huang, L., J. M. Regan, and X. Quan.** 2011. Electron transfer mechanisms, new applications, and performance of biocathode microbial fuel cells. Bioresource Technol. **102**:316–323.

27. **Jang, J. K., I. S. Chang, H. Moon, K. H. Kang, and B. H. Kim.** 2006. Nitrilotriacetic acid degradation under microbial fuel cell environment. Biotechnol. Bioeng. **95**:772–774.

28. **Jeffrey, S. W., and G. H. Humphrey.** 1975. New spectrophotometric equation for determining chlorophyll *a*, *b*, *c*1 and *c*2. Biochem. Physiol. Pflanz. **167**:194–204.

29. **Kim, B. H., H. J. Kim, M. S. Hyun, and D. H. Park.** 1999. Direct electrode reaction of Fe(III)-reducing bacterium, *Shewanella putrefaciens*. J. Microbiol. Biotechnol. **9**:127–131.

30. **Krammer, K., and H. Lange-Bertalot.** 1986-1991. Bacillariophyceae 1. Teil: Naviculaceae; 2. Teil: Bacillariaceae, Epithemiaceae, Surirellaceae; 3. Teil: Centrales, Fragilariaceae, Eunotiaceae; 4. Teil: Achnanthaceae. Kritische Ergänzungen zu *Navicula* (Lineolatae) und *Gomphonema*. *In* H. Ettl, J. Gerloff, H. Heynig, and D. Mollenhauer (ed.), Sußwasserflora von Mitteleuropa. Band 2/1–4, G. Fischer Verlag, Stuttgart, Germany.

31. **Kropf, S., H. Heuer, M. Grüning, and K. Smalla.** 2004. Significance test for comparing complex microbial community fingerprints using pairwise similarity measures. J. Microbiol. Meth. **57**:187–195.

32. **Lai, M. E., and A. Bergel.** 2000. Electrochemical reduction of oxygen by glassy carbon: catalysis by catalase. J. Electroanal. Chem. **494**:30–40.

33. **Landoulsi, J., K. El Kirat, C. Richard, D. Feron, and S. Pulvin.** 2008. Enzymatic approach in microbial-influenced corrosion: a review based on stainless steels in natural waters. Environ. Sci. Technol. **42**:2233–2242.

34. **Little, B., R. Ray, P. Wagner, Z. Lewandowski, W. C. Lee, W. G. Characklis, and F. Mansfeld.** 1991. Impact of biofouling on the electrochemical behaviour of 304 stainless steel in natural seawater. Biofouling **3**:45–59.

35. **Lock, M. A.** 1993. Attached microbial communities in rivers, p 113–138. *In* T. E. Ford (ed.), Aquatic microbiology - An ecological approach. Blackwell Scientific Publications, Oxford, UK.

36. **Logan, B. E.** 2009. Exoelectrogenic bacteria that power microbial fuel cells. Nature **7**:375–381.

37. **Lovley, D. R.** 2008. The microbe electric: conversion of organic matter to electricity. Curr. Opin. Biotech. **19**:564–571.

38. **Lozupone, C., and R. Knight.** 2005. UniFrac: a new phylogenetic method for comparing microbial communities. Appl. Environ. Microbiol. **71**:8228–8235.

39. **Lozupone, C., M. Hamady, and R. Knight.** 2006. UniFrac - An online tool for comparing microbial community diversity in a phylogenetic context. BMC Bioinformatics **7**:371.

40. **Lyautey, E., S. Teissier, J. Y. Charcosset, J. L. Rols, and F. Garabetian.** 2003. Bacterial diversity of phototrophic river biofilm assemblages of an anthropised river section, assessed by DGGE analysis of a 16S rDNA fragment. Aquat. Microb. Ecol. **33**:217–224.

41. **Lyautey, E., C. R. Jackson, J. Cayrou, J. L. Rols, and F. Garabetian.** 2005. Bacterial community succession in natural river biofilm assemblages. Microb. Ecol. **50**:589–601.

42. **Lyautey, E., B. Lacoste, L. Ten-Hage, J. L. Rols, and F. Garabetian.** 2005. Analysis of bacterial diversity in river biofilms using 16S rDNA PCR-DGGE: methodological settings and fingerprints interpretation. Water Res. **39**:380–388.

43. **Lyautey, E., S. Boulêtreau, E. Y. Madigou, and F. Garabetian.** 2010. Viability of differentiated epilithic bacterial communities in the River Garonne (SW France). Hydrobiologia **637**:207–218.

44. **Marconnet, C., C. Dagbert, M. Roy, and D. Féron.** 2008. Stainless steel enoblement in freshwater: from exposure tests to mechanisms. Corros. Sci. **50**:2342–2352.

45. **Mollica, A., E. Traverso, and D. Thierry.** 1997. On oxygen reduction depolarization induced by biofilm growth on stainless steel in sea water, p. 51–63. European Federation of Corrosion Publication No. 22. The Institute of Materials, London, UK.

46. **Mollica, A., and P. Cristiani.** 2003. On-line biofilm monitoring by "BIOX" electrochemical probe. Water Sci. Technol. **47**:45–49.

47. **Moon, H., I. S. Chang, J. K. Jang, K. S. Kim, J. Lee, R. W. Lovitt, and H. K. Byung.** 2005. On-line monitoring of low biochemical oxygen demand through continuous operation of a mediator-less microbial fuel cell. J. Microbiol. Biotechnol. **15**:192–196.

48. **Motoda, S., Y. Suzuki, T. Shinohara, and S. Tsujikawa.** 1990. The effect of marine fouling on the ennoblement of electrode potential for stainless steels. Corros. Sci. **31**:515–520.

49. **Normand, P., C. Ponsonnet, X. Nesme, M. Neyra, and P. Simonet.** 1996. ITS analysis of prokaryotes, p. 1–12. *In* D. L. Akkermans, J. D. van Elsas, and F. J. de Bruijn (ed.), Molecular microbial ecology manual. Kluwer Academic Publishers, Dordrecht, The Netherlands.

50. **Parot, S., O. Nercessian, M. L. Délia, W. Achouak, and A. Bergel.** 2009. Electrochemical checking of aerobic isolates from electrochemically active biofilms formed in compost. J. Appl. Microbiol. **106**:1350–1359.

51. **Parot, S., I. Vandecandelaere, A. Cournet, M. L. Délia, P. Vandamme, M. Bergé, C. Roques, and A. Bergel.** 2011. Catalysis of the electrochemical reduction of oxygen by bacteria isolated from electro-active biofilms formed in seawater. Bioresource Technol. **102**:304–311.

52. **Rabaey, K., S. T. Read, P. Clauwaert, S. Freguia, P. L. Bond, L. L. Blackall, and J. Keller.** 2008. Cathodic oxygen reduction catalyzed by bacteria in microbial fuel cells. ISME J. **2**:519–527.

53. **Rosenbaum, M., Z. He, and L. T. Angenent.** 2010. Light energy to bioelectricity: photosynthetic microbial fuel cells. Curr. Opin. Biotechnol. **21**:1–6.

54. **Rosenbaum, M., F. Aulenta, M. Villano, and L. T. Angenent.** 2011. Cathodes as electron donor for microbial metabolism: which extracellular electron transfers are involved? Bioresource Technol. **12**:324–333.

55. **Sabater, S., E. Navarro, and H. Guasch.** 2002. Effects of copper on algal communities at different current velocities. J. Appl. Phycol. **14**:391–398.

56. **Scotto, V., R. Dicintio, and G. Marcenaro.** 1985. The influence of marine aerobic microbial film on stainless-steel corrosion. Corros. Sci. **25**:185–194.

57. **Strik, D. P. B. T. B., H. Terlouw, H. V. M. Hamelers, and C. J. N. Buisman.** 2008. Renewable sustainable biocatalyzed electricity production in a photosynthetic algal microbial fuel cell (PAMFC). Appl. Microbiol. Biotechnol. **81**:659–668.

58. **Strik, D. P. B. T. B., H. V. M. Hamelers, and C. J. N. Buisman.** 2010. Solar energy powered microbial fuel cell with a reversible bioelectrode. Env. Sci. Technol. **44**:532–537.

59. **Ter Heijne, A., D. P. B. T. B. Strik, H. V. M. Hamelers, and C. J. N. Buisman.** 2010. Cathode potential and mass transfer determine performance of oxygen reducing biocathodes in microbial fuel cells. Environ. Sci. Technol. **44**:7151–7156.

60. **Tian, M., N. Kanavillil, L. Davey, K. T. Leung, H. Schraft, and A. Chen.** 2007. Direct growth of biofilms on an electrode surface and its application in electrochemical biosensoring. J. Electroanal. Chem. **611**:133–139.

61. **Tison, J., Y. S. Park, M. Coste, J. G. Wasson, L. Ector, F. Rimet, and F. Delmas.** 2005. Typology of diatom communities and the influence of hydro-ecoregions: a study on the French hydrosystem scale. Water Res. **39**:3177–3188.

62. **Vandecandelaere, I., O. Nercessian, M. Faimali, E. Segaert, A. Mollica, W. Achouak, P. De Vos, and P. Vandamme.** 2010. Biodiversity of the cultivable fraction of a marine electroactive biofilm. Bioelectrochemistry **78**:62–66

63. **Wasson, J. G., A. Chandesris, and H. Pella.** 2002. Définition des hydro-écorégions de France métropolitaine. Approche régionale de typologie des eaux courantes et éléments pour la définition des peuplements de référence d'invertébrés. Technical report, Cemagref Lyon BEA/LHQ, 190 pp.

64. **Wrighton, K. C., B. Virdis, P. Clauwaert, S. T. Read, R. A. Daly, N. Boon, Y. Piceno, G. L. Anderson, J. D. Coates, and K. Rabaey.** 2010. Bacterial community structure corresponds to performance during cathodic nitrate reduction. ISME J. **4**:1443–1455.

FIG. 1. Electrochemical potentials monitored during two *in situ* PRB colonization experiments at site U1 on 4 stainless steel replicate electrodes (black lines) and 2 replicate copper electrodes (grey lines) during 35 days in 2006 (a) and 18 days in 2007 (b). The data represents daily average of electrochemical potentials recorded every 30 min for each electrode.

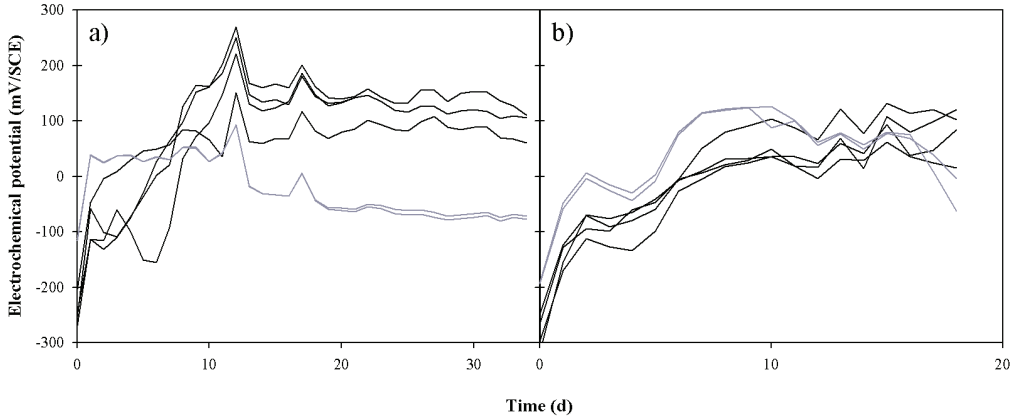

FIG. 2. Two dimensions MDS representation of distances between diatom communities from PRB grown at site U1 on stainless steel (black symbols) and copper (grey symbols) electrodes in 2006 (circles) and 2007 (triangles) (a), bacterial communities from PRB grown on stainless steel (black symbols) and copper (grey symbols) electrodes in 2006 and analyzed by PCR-DGGE (b), and bacterial communities from PRB grown on stainless steel (black symbols) and copper (grey symbols) electrodes in 2007 and analyzed by ARISA (c).

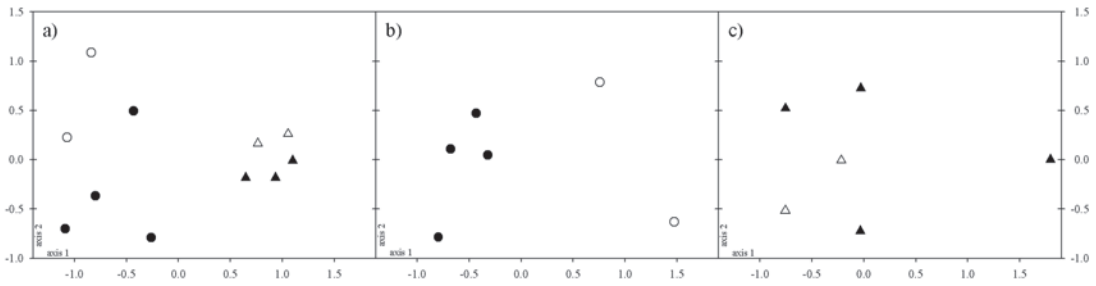

FIG. 3. Comparison of bacterial ARISA profiles from PRB sampled from sites U1 (a) and S (b) on natural supports. Data is peak height (fluorescence; Y axes) and fragment length (nucleotide base pairs; X axes), with profiles of both samples overlaid onto the same axis.

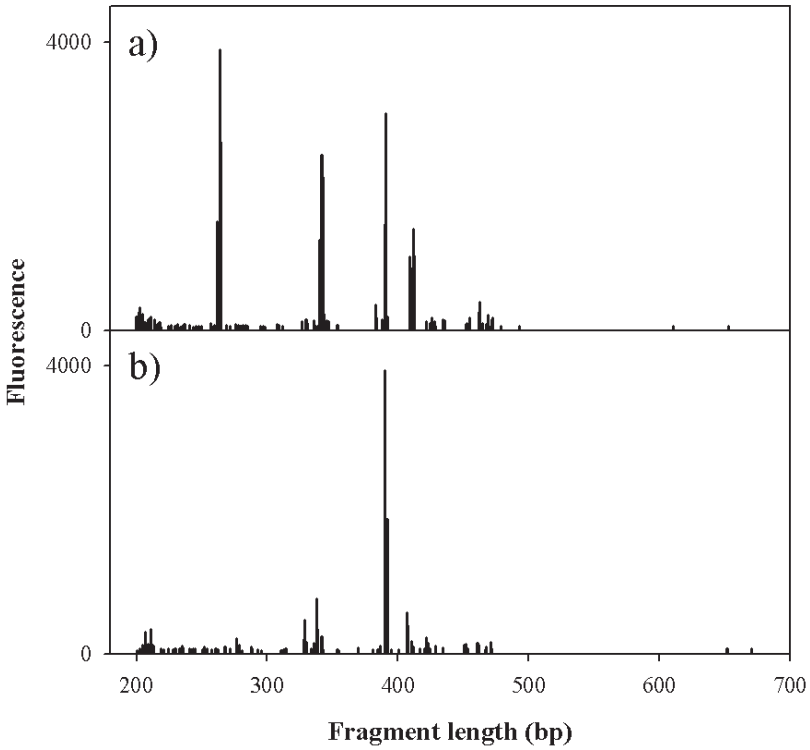

FIG. 4. Cyclic voltammograms obtained for a negative bacterial isolate (Site U1; GQ398344) (a), a moderately positive bacterial isolate (Site S; GQ398350) (b), and a positive bacterial isolate (Site U1; GQ398335) (c). Grey curve correspond to voltammograms obtained before cells injection, and black curve to voltammograms obtained after 3 h (a) and 1 h (b and c) of contact between the electrode and the bacterial suspension. Glassy carbon electrode, scan rate 100 mV s^{-1}.

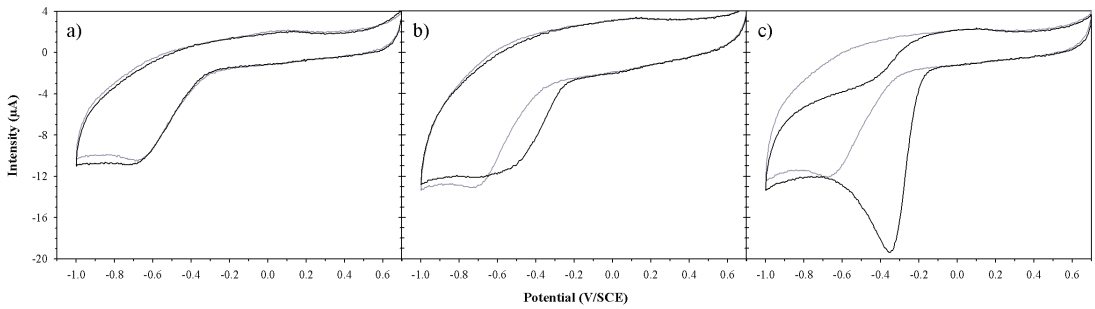

TABLE 1. Biochemical and voltammogram characteristics for the 32 strains tested in cyclic voltammetry. Accession number, site of origin, nearest relative identified based on 16S rRNA genes sequence analysis (with % of similarity), and results of Gram staining, catalase and oxidase tests, for the 32 bacterial strains tested in cyclic voltammetry. Shift of potential, peak amplitude and peak potential were obtained from the cyclic voltammetry experiments.

Accession no.	Site	Nearest relative (% similarity)	Gram	Catalase	Oxidase	Shift of potential (V)	Peak amplitude (µA)	Peak potential (V/SCE)
GQ398331	U1	*Citrobacter gillenii* (99.8)	–	+	–	0.15	–12.9	–0.48
GQ398332	U1	*Klebsiella oxytoca* (99.0)	–	+	–	0.22	–10.6	–0.49
GQ398333	U1	*Aeromonas sobria* (100)	–	–	+	0.12	–9.5	–0.49
GQ398334	U1	*Morganella morganii* (99.6)	–	+	–	0.18	–12.4	–0.54
GQ398335	U1	*Aeromonas sharmana* (97.4)	–	–	–	0.23	–19.4	–0.36
GQ398336	U1	*Acinetobacter johnsonii* (96.2)	–	+	–	0.09[a]	–11.6[a]	–0.61[a]
GQ398337	U1	*Microbacterium oxydans* (100)	–[b]	+	+	0.06[a]	[c]	[c]
GQ398338	U1	*Sphingomonas molluscorum* (98.6)	+/–	+	–	0.12	–10.4	–0.50
GQ398339	U1	*Moraxella osloensis* (99.9)	–	–	+	0.13[a]	[c]	[c]
GQ398340	U1	*Arthrobacter aurescens* (99.8)	–[b]	+	–	0.11	–13.3	–0.46

GQ398341 U1	*Exiguobacterium acetylicum* (99.9)	–[b]	+	–	0.16	–13.3	–0.49
GQ398342 U1	*Myroides odoratus* (99.5)	–	+	–	negative[a]	negative[a]	negative[a]
GQ398343 U1	*Pseudomonas fluorescens* (99.8)	–	+	+	0.14	–14.6	–0.47
GQ398344 U1	*Massilia timonae* (99.5)	–	–	+	negative[a]	negative[a]	negative[a]
GQ398345 U1	*Rhodococcus equi* (100)	+	–	+	0.09[a]	–11.3[a]	–0.64[a]
GQ398347 S	*Rhizobium radiobacter* (99.6)	–	+	–	0.10[a]	[c]	[c]
GQ398350 S	*Variovorax paradoxus* (99.6)	–	+	+	0.14	–11.3	–0.54
GQ398351 S	*Chryseobacterium ureilyticum* (99.5)	+[b]	+	–	0.13	–11.3	–0.51
GQ398353 S	*Flavobacterium johnsoniae* (99.0)	–	+	+	0.06[a]	–12.5[a]	–0.76[a]
GQ398355 S	*Exiguobacterium sibiricum* (99.9)	–[b]	+	+	0.14	–10.5	–0.50
GQ398356 S	*Exiguobacterium undae* (99.7)	–[b]	+	+	0.13	–12.6	–0.42
GQ398357 S	*Novosphingobium aromaticivorans* (97.7)	–	+	+	negative[a]	negative[a]	negative[a]
GQ398359 S	*Bacillus cereus* (99.9)	+	+	–	negative[a]	negative[a]	negative[a]
GQ398360 S	*Bacillus flexus* (100)	–[b]	+	–	0.11	[c]	[c]
GQ398364 S	*Raoultella terrigena* (100)	–	+	–	0.12	–10.8	–0.54
GQ398367 S	*Curtobacterium flaccumfaciens* (99.8)	+	+	–	negative[a]	negative[a]	negative[a]
GQ398368 S	*Labedella kawkjii* (99.8)	+	+	–	negative[a]	negative[a]	negative[a]

GQ398369	S	*Frigoribacterium faeni* (99.5)	+	+	–	0.20[a]	–14.5[a]	–0.48[a]
GQ398370	S	*Leucobacter luti* (98.7)	–[b]	+	–	negative[a]	negative[a]	negative[a]
GQ398373	S	*Pseudomonas putida* (100)	+[b]	+	+	0.22	–14.5	–0.45
GQ398374	S	*Janthinobacterium lividum* (99.9)	–	+	+	0.18	–11.9	–0.52
GQ398375	S	*Zoogloea ramigera* (98.7)	–	+	+	0.13[a]	–11.0[a]	–0.52[a]

[a] Values recorded after a 3-h contact time.

[b] The observed Gram is different from expected based on the nearest relative of the tested isolate.

[c] Small catalytic effect observed but no clear peak.

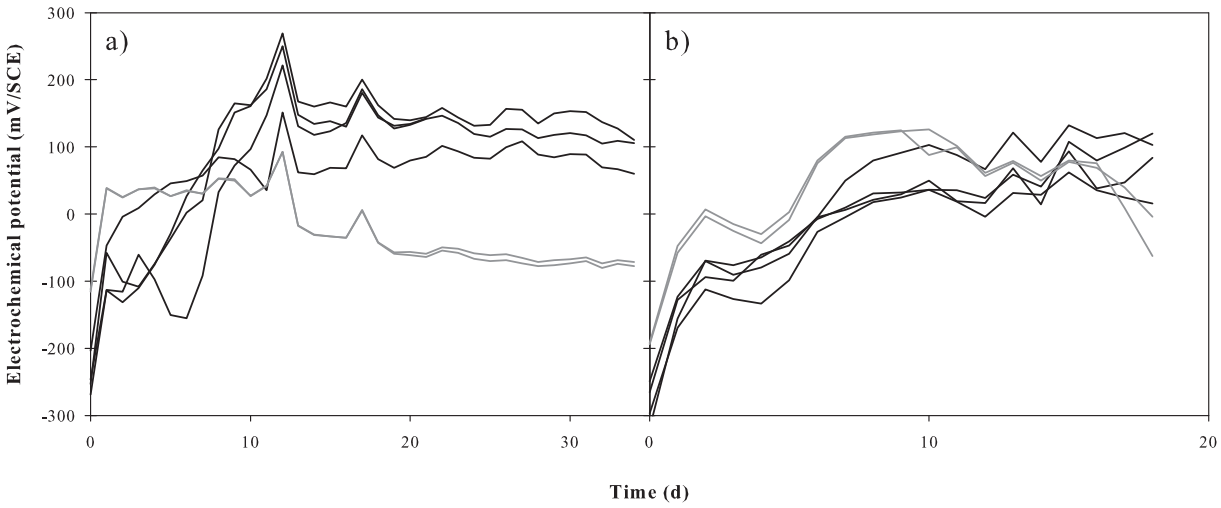
a)
b)
Electrochemical potential (mV/SCE)
300
200
100
0
-100
-200
-300
0
10
20
30
0
10
20
Time (d)

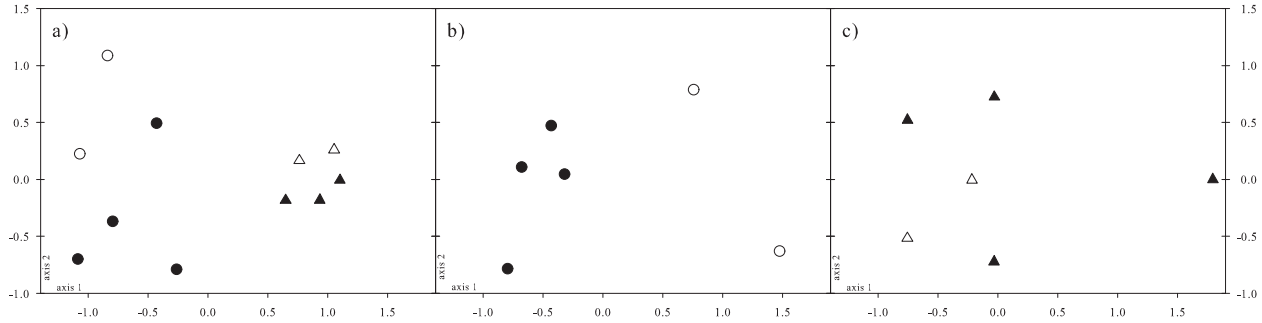
a)
b)
c)
axis 1
axis 2
1.5
1.0
0.5
0.0
-0.5
-1.0
-1.0
-0.5
0.0
0.5
1.0
1.5

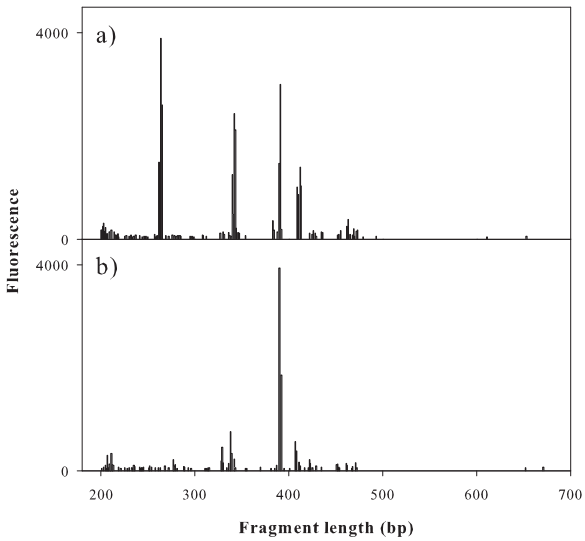
a)
b)
4000
0
4000
0
Fluorescence
200
300
400
500
600
700
Fragment length (bp)

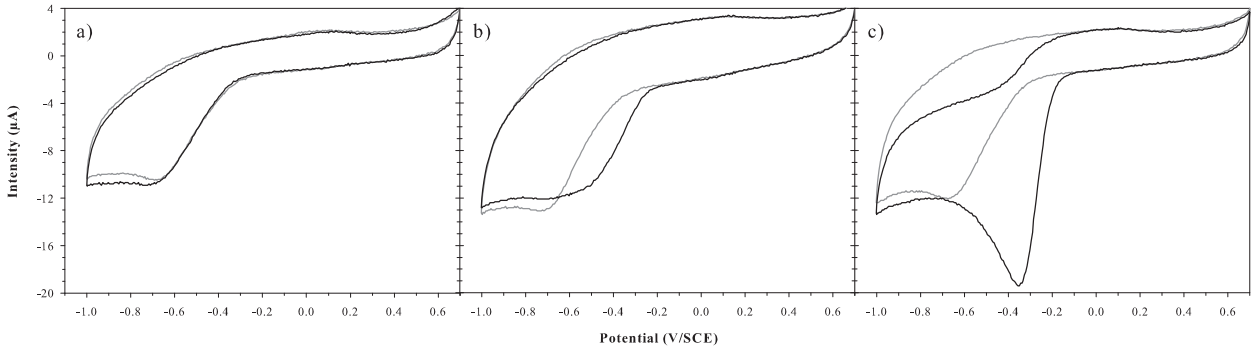
a)
b)
c)
Intensity (µA)
Potential (V/SCE)
4
0
-4
-8
-12
-16
-20
-1.0
-0.8
-0.6
-0.4
-0.2
0.0
0.2
0.4
0.6